Journal of the European Ceramic Society 21 (2001) 245–250

www.elsevier.com/locate/jeurceramsoc

Plastic deformation of silicon nitride/boron nitride fibrous monoliths

A.R. de Arellano-López [a,*], S. López-Pombero [a], A. Domínguez-Rodríguez [a], J.L. Routbort [b], D. Singh [b], K.C. Goretta [b]

[a] *Departamento de Fisica de la Materia Condensada, Universidad de Sevilla, PO Box 1065, 41080 Seville, Spain*
[b] *Energy Technology Division, Argonne National Laboratory, Argonne, IL 60349-4838, USA*

Received 27 November 1999; received in revised form 31 May 2000; accepted 11 June 2000

Abstract

High-temperature compressive creep of unidirectional Si_3N_4/BN fibrous monoliths has been investigated at 1300–1500°C in an inert atmosphere. The results were then compared to those for deformation of the Si_3N_4 and BN base materials. Plasticity of the fibrous monoliths was limited to very low stresses when the Si_3N_4 cells were oriented perpendicular to the stress axis because the BN cell boundaries failed, followed by failure of the Si_3N_4 cells. In the fibrous monolith in which cells were oriented parallel to the stress axis, steady-state deformation controlled by deformation of the Si_3N_4 cells was achieved.

Keywords: Creep; BN; Fibrous monoliths; Mechanical properties; Si_3N_4

1. Introduction

Ceramic fibrous monoliths generally consist of strong ceramic cells that are surrounded by a weaker cell boundary (see schematic diagram in Fig. 1a). These monoliths are produced from ceramic powders by conventional fabrication techniques, such as extrusion.[1,2] They exhibit graceful failure; in flexure, they splinter.[1–5] In many applications, fibrous monoliths may offer a low-cost alternative to conventional continuous-fiber ceramic composites.

Several compositions of ceramics and cermets have been processed successfully in fibrous monolithic form.[4] The most thoroughly investigated fibrous monolith consists of Si_3N_4 cells and a continuous BN cell boundary.[3–5] Through appropriate selection of initial powders, and extrusion and hot-pressing parameters, strong, very tough Si_3N_4/BN products have been produced.[2–7] The high toughness is due primarily to crack deflection along the weaker BN phase.

Fracture of Si_3N_4/BN fibrous monoliths has been studied extensively at both room and high temperatures.[3–11] However, very little effort has focused on creep.[9,10] Fracture testing of Si_3N_4/BN fibrous monoliths in air at temperatures up to 1400°C has indicated that shear failures become dominant at 1100°C and above and that creep of the Si_3N_4 phase becomes significant at ≈1400°C.[11] The creep rates have not been quantified.

We report here on compressive creep of Si_3N_4/BN fibrous monoliths that were tested in inert atmosphere. For comparison, Si_3N_4 and BN specimens with compositions similar to those of the components of the fibrous monolith phase were also tested.

2. Experimental details

2.1. Specimen fabrication

The fibrous monoliths were produced by Advanced Ceramics Research of Tucson, AZ. They were fabricated from ≈325-μm-diameter Si_3N_4/BN coextruded green filaments[5] that were produced by melt coextrusion of a blend of ≈52 vol.% ceramic powder mixture in an ethylene-based copolymer binder.[11] The coextruded filaments contained nominally 85 vol.% core Si_3N_4 material (E-10, Ube Industries, Tokyo) and 15 vol.% BN cladding (HCP Grade, Advanced Ceramics Corporation, Cleveland). The Si_3N_4 was of a sinterable composition, 92 wt.% commercial Si_3N_4 powder, 6

* Corresponding author. Tel.: +34-95-4552891; ext. 96; fax: +34-95-4612097.
E-mail address: ramirez@cica.es (A.R. de Arellano-López).

0955-2219/01/$ - see front matter
PII: S0955-2219(00)00175-8

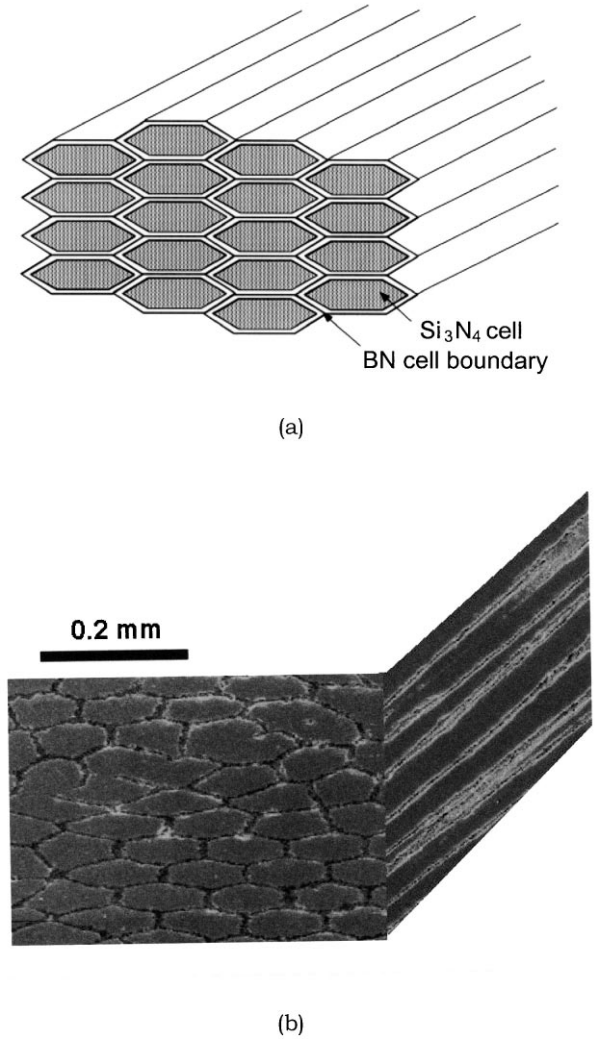

Fig. 1. (a) Schematic diagram of the structure of the fibrous monoliths; (b) SEM photomicrographs showing the structure of the materials in this study.

wt.% Y_2O_3, and 2 wt.% Al_2O_3. The oxides were added to promote densification.

Single-filament-thick sheets of uniaxially aligned green filaments were produced by a winding operation that placed the coextruded filaments side by side on a cylindrical mandrel. The filaments were held in place with a spray adhesive that, upon drying, allowed removal of the unidirectional sheets of green fibrous monolith from the mandrel. The sheets were stacked to fabricate unidirectional, 0° specimens.[5] Although Advanced Ceramics Research can produce complex laminated architectures, only 0° specimens were examined. The laminates were cut into the desired preform and warm pressed at 160°C to produce a solid green panel.

Simple, rectangular, flat panels were fabricated and subjected to a binder pyrolysis step that consisted of slow heating in flowing N_2 to 600°C over a period of 42 h. The panels were then uniaxially hot pressed at 1740°C for 1 h under ≈28 MPa pressure. This procedure yielded fibrous-monolith billets with densities >98% of their theoretical density. During hot pressing, some of the oxide additives to the Si_3N_4 diffused into the BN.[11,12] The final structure of the material is documented in the scanning electron photomicrograph montage in Fig. 1b.

By similar techniques, monolithic Si_3N_4 and BN billets were also hot pressed from extruded filaments. Each monolithic ceramic also contained Y_2O_3 and Al_2O_3 in the approximate concentrations that are found in the phases of the Si_3N_4/BN fibrous monoliths.[12,13]

2.2. Creep tests and microstructural analyses

Right parallelepiped specimens ≈3×3×5 mm were cut from the fibrous-monolith and Si_3N_4 billets with a slow-speed diamond-blade saw. Si_3N_4 and BN specimens were also prepared; the BN was cut parallel (BNpara) and perpendicular (BNperp) to the extrusion direction. Fibrous monoliths were also cut parallel (FMpara) and perpendicular (FMperp) to the axis of the filaments. All compression surfaces were polished to be flat and parallel.

Both constant-strain-rate (CSR) and constant-load (CL) tests were conducted. The purpose of the CSR tests was to assess the likely ranges of plasticity. In these tests, each specimen was compressed at constant velocity between Si_3N_4 platens in an Instron Model 1125 universal tester.[10,14] The atmosphere was static N_2, the temperature was 1300–1500°C, and the engineering strain rates ($\dot{\varepsilon}$) were ≈1×10^{-6}–5×10^{-6} s^{-1}. All CSR tests were completed within 10 h. For most tests, the specimens were unloaded and reloaded and at least two data points were taken for apparent steady-state stress (σ).

CL tests were conducted in a dead-load prototype apparatus that has been described.[15] A static Ar atmosphere was used, and temperatures from 1400 to 1500°C were selected. Based on previous high-temperature fracture studies,[11] creep of Si_3N_4/BN fibrous monoliths should be relatively rapid in this temperature range. CL testing allowed for measurement of a wide range of stresses (10–200 MPa), and calculation of creep parameters from load and temperature changes.

The microstructures of the undeformed and deformed specimens were analyzed by optical and scanning electron microscopy (SEM). The BN grains were platelike; the Si_3N_4 grains exhibited large aspect ratios, with average dimensions of ≈1×4 μm.[10] Morphological changes of the cells were studied with an image analyzer (Zeiss Videoplan). Microstructural evolution during deformation was correlated to deformation mechanisms.

3. Results and discussion

CSR tests were performed on BNpara and BNperp samples. As seen in Fig. 2, apparent steady-state stresses were higher for the BNpara samples than for the

BNperp samples. Apparent stresses were essentially independent of temperature and strain rate. SEM revealed, however, that the deformation of the BN samples was dominated by sequential fracture (Fig. 3). As has also been observed in creep testing of high-temperature Bi-based cuprate superconductors, which consist of platelike grains, apparent steady-state responses can be obtained, but deformation actually proceeds by bending of the grains with concomitant microcracking between grains.[16] The finding of creep fracture, rather than steady-state creep, in these CSR tests was not surprising. Torsional creep experiments achieved steady-state deformation only at temperatures $>2000^{\circ}C$.[17] The fact that the fracture stress was approximately independent of temperature over the narrow range used in these tests is expected.

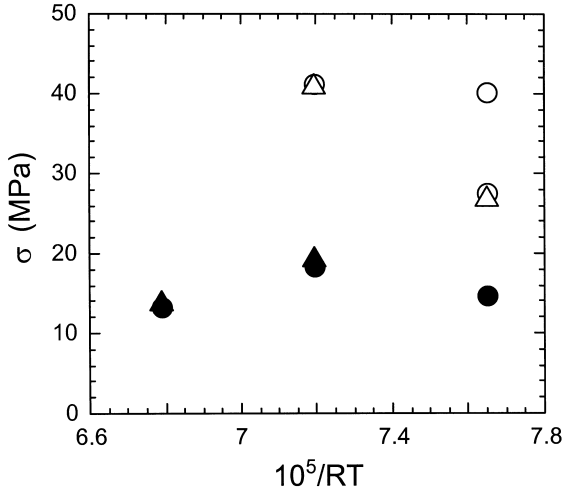

Fig. 2. Apparent steady-state stresses from CSR tests on extruded BN: ○, BNpara, $\dot{\varepsilon}=2\times10^{-6}$ s^{-1}; △, BNpara, $\dot{\varepsilon}=1\times10^{-6}$ s^{-1}; ●, BNperp, $\dot{\varepsilon}=2^{-}10^{-6}$ s^{-1}; ▲ BNperp, $\dot{\varepsilon}=1\times10^{-6}$ s^{-1}.

A summary of all of the creep tests that were performed on the FM and Si_3N_4 samples is shown as a log–log plot in Fig. 4. The data points in this figure correspond to the range in which apparent steady states were measured. Below the minimum stress for each material, no deformation was recorded; above the maximum values, the high stresses led to accelerating deformation (i.e. tertiary creep). For comparison, the BN results have also been included. Over the experimental temperature range, BN is substantially softer than the Si_3N_4 and FM samples and does not deform in the steady-state, as noted above.

The FMperp samples did not undergo significant plastic deformation under the testing conditions. At 1400°C, only two data points were recorded, at 12 and

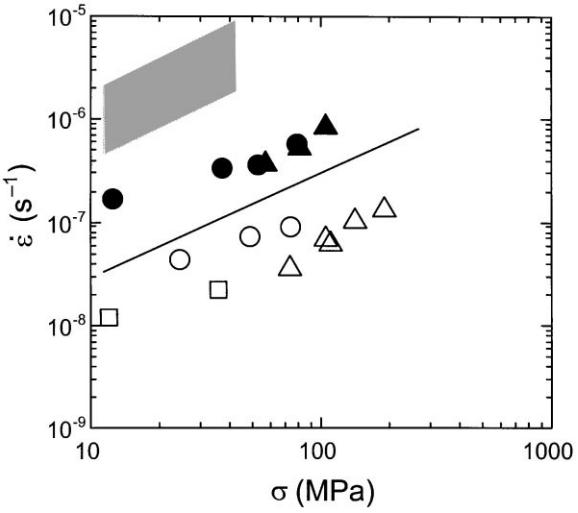

Fig. 4. CL tests on Si_3N_4 monoliths and FMs. The symbols are: ○, Si_3N_4 — 1400°C; ●, Si_3N_4 — 1500°C; △, FMpara — 1400°C; ▲, FMpara — 1500°C; □, FMperp — 1400°C. The slope of the line is 1; the shaded region indicates range of BN response.

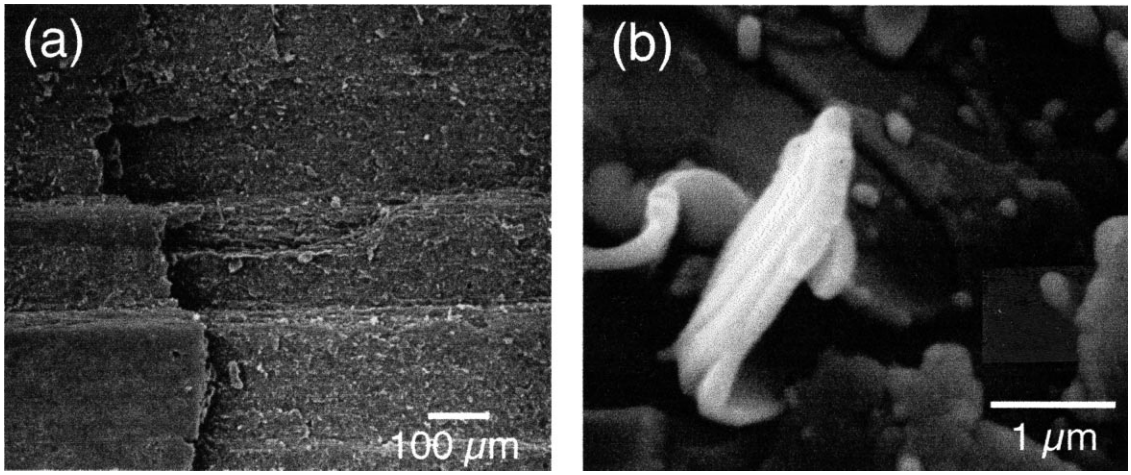

Fig. 3. SEM photomicrographs, showing fracture of BN from deformation: (a) low-magnification view and (b) high-magnification view, in which cleavage and bending of BN grains are evident.

40 MPa, before fracture occurred at only 0.7% strain. This orientation was extremely brittle. The cracked BN matrix could not prevent the sliding of the Si_3N_4 cells, and fracture occurred, primarily by propagation of a single intercell crack, along a diagonal of the section perpendicular to the cells (Fig. 5). On the other hand, the FMpara and Si_3N_4 samples deformed ≈10% without fracture.

The FMpara samples did not deform in steady state under lower stresses. For those stresses, the only significant feature was cracking within the BN matrix, until the load was fully transferred to the Si_3N_4 cells. At 1400°C, the first apparent steady-state was measured under 75 MPa; at 1500°C, the lowest stress that yielded a steady-state was 57 MPa. Once a critical stress was surpassed and the load could be transferred to the cells, they deformed plastically and controlled the deformation.

The monolithic Si_3N_4 deformed in steady state at 1500°C at stresses as low as 13 MPa. At higher stresses, the agreement between the absolute creep rates of the FMpara and Si_3N_4 monolith was outstanding, because for both types of samples, the creep rate was controlled by the deformation of the polycrystalline Si_3N_4.

This conclusion was confirmed by studying the evolution of the sections of the cells of the FMpara samples during creep. The equivalent diameter of the undeformed cells was 103.0±2.3 μm. A 3940-μm-long sample was deformed to a final length of ≈3500 μm. A morphological study was performed on a section of this sample (Fig. 6a). SEM photomicrographs revealed intercell cracks; however, the sample did not fail. The cracks within the BN phase were due to buckling of the cells, mostly those nearest the surface (Fig. 6b).

If one assumes a constant cell volume,

$$S_f = S_o(l_o/l_f) \tag{1}$$

and

$$D_f = D_o\sqrt{l_o/l_f}\ ,$$

where D, S, and l refer to the diameter, area, and length of a cell and the subscripts o and f refer to the initial and final dimensions, respectively. Based on constant cell volume, the final average diameter of the cells was calculated to be 109.2 μm. The measured value was 110.0±1.7 μm, in excellent agreement with the calculated value.

For analysis of the creep data, a classical semi-phenomenological equation was used,[18]

$$\dot{\varepsilon} = A\sigma^n e^{-Q/RT}\ , \tag{2}$$

where $\dot{\varepsilon}$ is the strain rate, σ is stress, T is absolute temperature, n and Q are adjustable parameters, A is a constant, and R is the gas constant.

Fig. 4 indicates that the dependence of strain rate on stress is approximately linear ($n \approx 1$); thus, a more-detailed understanding can be achieved by plotting the data on a linear-linear graph (Fig. 7). The regression lines are reasonable; both were selected to intersect the origin. The slopes of the regression lines at $T_1 = 1400$°C

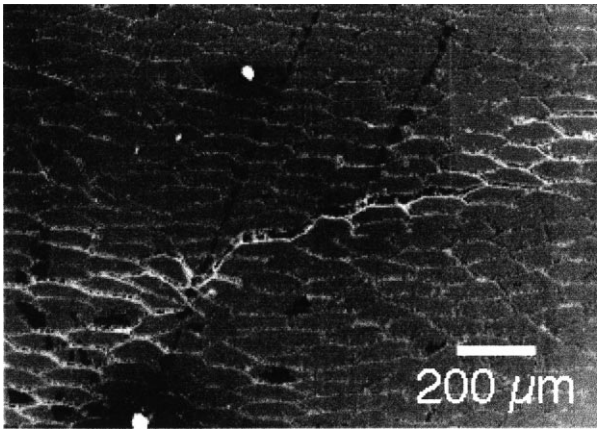

Fig. 5. SEM photomicrograph of deformed FMperp sample, showing formation of damage that led to failure; in the figure the compression axis was horizontal.

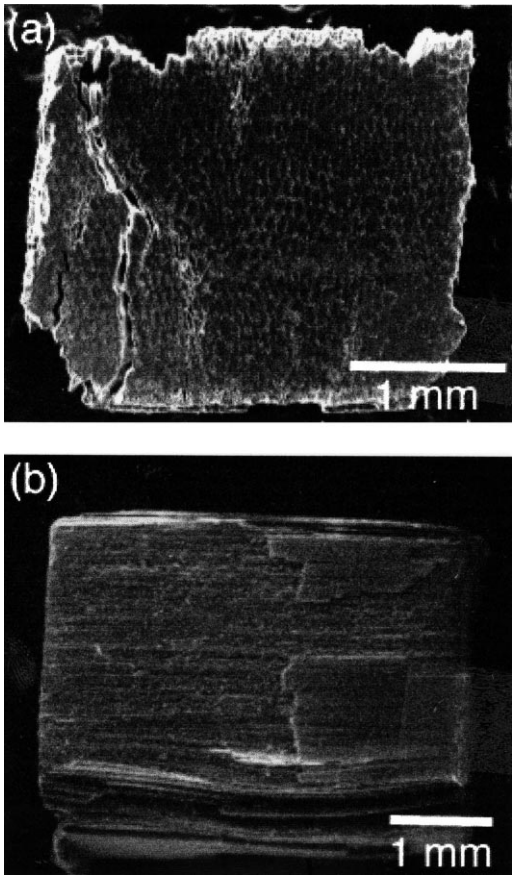

Fig. 6. SEM photomicrographs of deformed FMpara sample: (a) sections of cells and (b) buckling of cells that were near the surface; in the figure the compression axis was horizontal.

($B_1 = 7.6710\times10^{-10}$ MPa^{-1} s^{-1}) and $T_2 = 1500°C$ ($B_2 = 7.7903\times10^{-9}$ MPa^{-1} s^{-1}) can be used to obtain an estimate of the activation energy as follows:

$$\frac{e^{-Q/RT_1}}{e^{-Q/RT_2}} = \frac{B_1}{B_2} \quad \Rightarrow \quad Q = \frac{RT_1T_2}{T_1 - T_2}\ln\left(\frac{B_1}{B_2}\right). \tag{3}$$

Eq. (3) yields $Q = 570\pm150$ kJ/mol. A specific experiment to determine Q directly was performed by temperature jumps between 1400 and 1500°C on a FMpara sample, under a constant stress of 105 MPa (Fig. 8). The result was $Q = 625\pm40$ kJ/mol, which is in fair agreement with the Q value calculated when all of the data points are considered.

These values for n and Q, are in excellent agreement with previous work on Si_3N_4 that contained a grain-boundary phase.[19–24] Several authors have suggested that compressive creep occurs by grain-boundary sliding probably accommodated by solution/reprecipitation of the Si_3N_4 phase and viscous flow of the boundary phase.[19–24]

It was determined that the polycrystalline Si_3N_4 phase controls the creep-rate of the parallel-orientation FMs. This conclusion is similar to that obtained from creep of unidirectional SiC-fiber/mullite composites.[25] In general, creep of unidirectional FMs is likely to be dominated by the weaker, cell-boundary phase when compression is perpendicular to the cells and dominated by the stronger cells when compression is parallel to the cells.

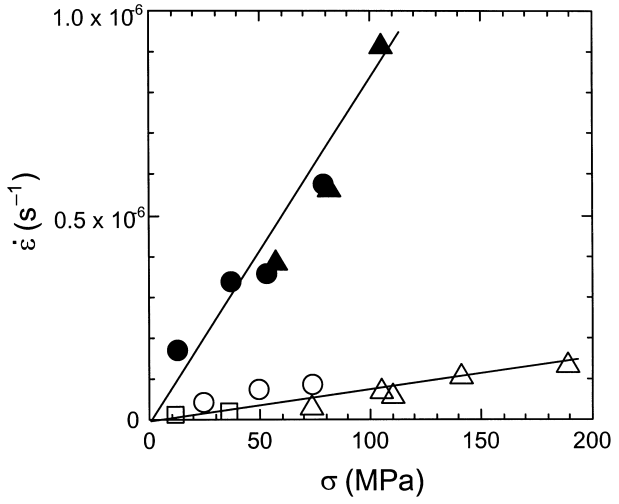

Fig. 7. CL creep results on a linear–linear graph; ○,△ = 1400°C and ●,▲ = 1500°C.

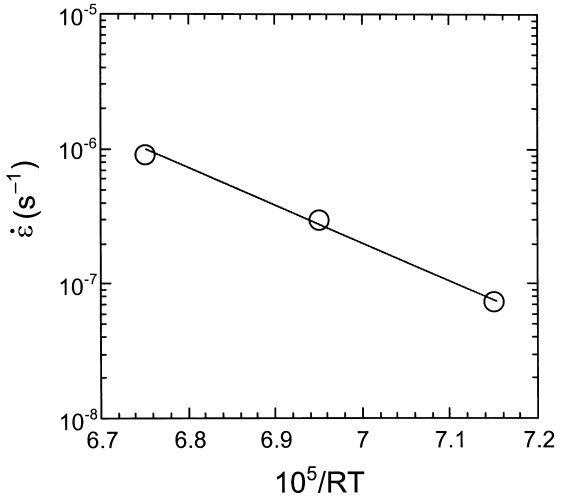

Fig. 8. CL test to determine $Q = 625\pm40$ kJ/mol for FMpara sample; stress = 105 MPa.

4. Conclusions

Compressive creep of a unidirectional Si_3N_4/BN fibrous monoliths and its individual constituents, BN and Si_3N_4, was investigated in inert atmosphere at 1300–1500°C. When the cells in the fibrous monolith were oriented perpendicular to the stress axis, steady-state deformation was limited to very low stresses. For this orientation, fracture of the BN matrix occurred, followed by fracture of the Si_3N_4 cells. When the cells in the fibrous monolith were oriented parallel to the stress axis, steady-state deformation and permanent strains to 10% were achieved. In this orientation, plastic deformation was controlled by deformation of the Si_3N_4 cells.

Acknowledgements

We thank M. Rigali and M. Sutaria for supplying the test materials. This work was supported in Sevilla by the Spanish Ministerio de Educación, CICYT Project MAT97-1007-C02, and at Argonne National Laboratory by the Defense Advanced Research Projects Agency, through a Department of Energy Interagency Agreement, under Contract W-31-109-Eng-38. J.L.R. is grateful to IBERDROLA for providing funds during his stay at the University of Sevilla.

References

1. Coblenz, W. S. Fibrous monolithic ceramic and method for production. US Patent 4,772,524, 20 September 1988.
2. Popovich, D., Halloran, J. W., Hilmas, G. E., Brady, G. A., Somas, S., Bard, A. and Zywicki, G. Process for preparing textured ceramic composites. US Patent. 5,645,781, 8 July 1997.
3. Hilmas, G., Brady, G. A., Abdali, U., Zywicki, G. and Halloran, J., Fibrous monoliths: non-brittle fracture from powder-processed ceramics. *Mater. Sci. Eng.*, 1995, **A195**, 263–268.
4. Kovar, D., King, B. H., Trice, R. W. and Halloran, J. W., Fibrous monolithic ceramics. *J. Am. Ceram. Soc.*, 1997, **80**, 2471–2487.

5. Danko, G. A., Hilmas, G. E., Halloran, J. W. and King, B., Fabrication and properties of quasi-isotropic silicon nitride-boron nitride fibrous monoliths. *Ceram. Eng. Sci. Proc.*, 1997, **18**(3), 607–613.
6. Popovich, D., Danko, G. A., Hilmas, G. E., Stuffle, K., King, B. H., Brady, G. A., Trice, R. W. and Halloran, J. W., Fibrous monoliths: room- and high-temperature non-brittle fracture from powder processed ceramics. *Ceram. Eng. Sci. Proc.*, 1996, **17**(3), 278–286.
7. Kovar, D., Thouless, M. D. and Halloran, J. W., Crack deflection and propagation in layered silicon nitride/boron nitride ceramics. *J. Am. Ceram. Soc.*, 1998, **81**, 1004–1012.
8. Lee, S. W. and Kim, D. K., High-temperature characteristics of Si_3N_4/BN fibrous monolithic ceramics. *Ceram. Eng. Sci. Proc.*, 1997, **18** (4), 481–486.
9. Zawada, L. AFRL/MLLN, Wright-Patterson Air Force Base, unpublished information, 1998.
10. Routbort, J. L., Goretta, K. C., Park, E. T., Singh, D., Finch, J., Staehler, J., Zawada, L. and Hilmas, G. E., High-temperature compressive deformation of Si_3N_4/BN fibrous monoliths. *Ceram. Eng. Sci. Proc.*, 1999, **20**(3), 427–434.
11. Trice, R. W. and Halloran, J. W., The elevated temperature mechanical properties of silicon nitride/boron nitride fibrous monolithic ceramics. *J. Am. Ceram. Soc.*, 2000, **83**, 311–316.
12. Trice, R. W. and Halloran, J. W., Influence of microstructure and temperature on the interfacial fracture energy of silicon nitride/boron nitride fibrous monolithic ceramics. *J. Am. Ceram. Soc.*, 1999, **82**, 2502–2508.
13. Rigali, M. Advanced Ceramics Research, Tucson, AZ, private communication, 1999.
14. de Arellano-López, A. R., Smirnov, B. I., Goretta, K. C. and Routbort, J. L., Creep of an Al_2O_3–SiC(whisker)–TiC(particle) composite. *Mater. Sci. Eng.*, 1998, **A252**, 93–97.
15. Gervais, H., Pellisier, B. and Castaing, J., Machine de fluage pour essais en compression a hautes temperatures de materieus ceramiques. *Int. Hautes Temp. Refract.*, 1978, **15**, 43–47.
16. Goretta, K. C., Zamirowski, E. J., Calderon-Moreno, J. M., Miller, D. J., Chen, N., Holesinger, T. G. and Routbort, J. L., High-temperature deformation and fracture of Bi–Sr–Ca–Cu–O superconductors. *J. Mater. Res.*, 1994, **9**, 541–547.
17. Pezzotti, G., Kleebe, J.-J., Ota, K. and Nishida, T., Internal friction and torsional creep behavior of chemically vapor deposited boron nitride. *J. Mater. Res.*, 1998, **13**, 3453–3457.
18. Cannon, W. R. and Langdon, T. G., Review: creep of ceramics, part 1. Mechanical characteristics. *J. Mater. Res.*, 1983, **18**, 1–50.
19. Ziegler, G., Heinrich, G. and Wötting, G., Review: relationships between processing, microstructure and properties of dense and reaction-bonded silicon nitride. *J. Mater. Sci.*, 1987, **22**, 3041–3086.
20. Raj, R. and Morgan, P. E. D., Activation energies for densification, creep, and grain-boundary sliding in nitrogen ceramics. *J. Am. Ceram. Soc.*, 1981, **64**, C143–C145.
21. Clarke, D. R., High-temperature microstructure of a hot-pressed silicon nitride. *J. Am. Ceram. Soc.*, 1989, **72**, 1604–1609.
22. Luecke, W. E., Wiederhorn, S. M., Hockey, B. J., Krause, R. F. Jr and Long, G. G., Cavitation contributes substantially to tensile creep in silicon nitride. *J. Am. Ceram. Soc.*, 1995, **78**, 2085–2096.
23. Dryden, J. R., Kucerovsky, D., Wilkinson, D. S. and Watt, D. F., Creep deformation due to a viscous grain boundary phase. *Acta Metall.*, 1989, **37**, 2007–2015.
24. Dryden, J. R. and Wilkinson, D. S., Three dimensional analysis of the creep due to a viscous grain boundary phase. *Acta Metall. Mater.*, 1997, **45**, 1259–1273.
25. Deng, Z.-H. and Kobayashi, T., Compressive creep behavior of SiC fiber-reinforced mullite matrix composites. *Ceram. Eng. Sci. Proc.*, 1998, **22**(3), 129–136.